ACS Energy LETTERS

http://pubs.acs.org/journal/aelccp

FOCUS REVIEW

From Atoms to Cells: Multiscale Modeling of $LiNi_xMn_yCo_zO_2$ Cathodes for Li-Ion Batteries

Lucy M. Morgan, Mazharul M. Islam, Hui Yang, Kieran O'Regan, Anisha N. Patel, Abir Ghosh, Emma Kendrick, Monica Marinescu, Gregory J. Offer, Benjamin J. Morgan, M. Saiful Islam, Jacqueline Edge,* and Aron Walsh*

Cite This: *ACS Energy Lett.* 2022, 7, 108−122

Read Online

ACCESS | Metrics & More | Article Recommendations

ABSTRACT: First-generation cathodes for commercial lithium-ion batteries are based on layered transition-metal oxides. Research on ternary compounds, such as $LiCoO_2$, evolved into mixed-metal systems, notably $Li(Ni,Mn,Co)O_2$ (NMCs), which allows significant tuning of the physical properties. Despite their widespread application in commercial devices, the fundamental understanding of NMCs is incomplete. Here, we review the latest insights from multiscale modeling, bridging between the redox phenomena that occur at an atomistic level to the transport of ions and electrons across an operating device. We discuss changes in the electronic and vibrational structures through the NMC compositional space and how these link to continuum models of electrochemical charge−discharge cycling. Finally, we outline the remaining challenges for predictive models of high-performance batteries, including capturing the relevant device bottlenecks and chemical degradation processes, such as oxygen evolution.

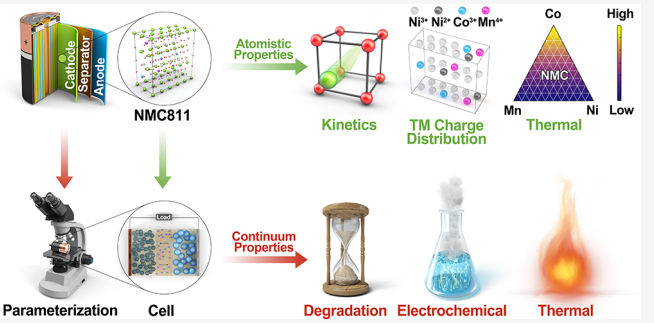

Lithium-ion batteries (LIBs) were developed by Whittingham in the 1970s[1,2] but did not become a promising technology until 1979, when Goodenough and Mizushima successfully demonstrated $LiCoO_2$ as a cathode and Yoshino developed an anode based on carbon instead of reactive lithium.[3] These were successfully commercialized by Sony in 1991, and have since become instrumental in portable electronics, electric vehicles, and grid storage applications.[4−10] However, to fully electrify the transport and energy sectors, further advancements in LIBs are required to achieve higher energy densities, better longevity, and lower cost from sustainable materials. The performance of a battery is highly dependent on the choice of cathode material and the transition metals from which they are composed.[11−14]

$LiCoO_2$ offers a number of attractive features, including ease of synthesis, reversible lithium insertion, high specific energy density, and high thermal stability.[15−17] However, its application was limited due to capacity fade and the cost/geopolitical issues of cobalt mining, which made large-scale energy storage solutions impractical.[18,19] Other oxide materials were considered, such as $LiNiO_2$ and $Li_xMn_2O_4$, each with its own challenges, such as the longevity and safety of $LiNiO_2$[20] and $Li_xMn_2O_4$ showing irreversible structural changes due to strong Jahn−Teller effects and low capacity.[21] Partial replacement of Co in $LiCoO_2$ with Ni and Mn was considered, resulting in the layered oxide $LiNi_xMn_yCo_zO_2$ (where $x + y + z = 1$), commonly termed NMCs, often followed by numbers relating to the ratio of the transition metals.[9,22−24] These NMC materials were able to achieve a more balanced performance, preserving favorable voltage characteristics, reaching a higher capacity (200 mAh g^{-1}), and addressing cost and abundance issues.[25−27] NMCs also demonstrate improved electrochemical performance, enhanced rate capability,[17,28] and better cycle life/thermal stability.[29,30]

The tuning of the transition-metal compositions of NMCs has been a focus of research, in an effort to optimize desirable battery properties including capacity, cyclic rate, electrochemical stability, and lifetime while also reducing cost.[31] Many NMC compositions are already in use, with commercial

Received: September 19, 2021
Accepted: November 17, 2021

https://doi.org/10.1021/acsenergylett.1c02028
ACS Energy Lett. 2022, 7, 108−122

applications shifting from NMC111 to higher Ni compositions, including NMC811 ($LiNi_{0.8}Mn_{0.1}Co_{0.1}O_2$).[32] Current investigations are now focused toward further reducing the Co content and optimizing Ni-rich compositions, such as NMC811, to improve the performance of current and future generation batteries for long-range electric vehicles[33] and for use in all-solid-state LIBs.[24,25,27,34−36]

Despite the improved properties of Ni-rich NMCs, these materials still exhibit rapid voltage and capacity fading, as well as poor structural and thermal stability,[17,37,38] leading to severe degradation.[31,39−43] Degradation can occur through a range of physical and chemical processes, resulting in loss of lithium inventory (LLI), loss of active material (LAM), and/or impedance increase.[44] Attempts have been made to circumvent these degradation processes using approaches including surface coating, doping with ions, and electrolyte modification;[11,45] however, current experimental probes are limited in the detail they can provide. Additional challenges lie in improving the safety and prolonging the life of batteries, requiring optimal thermal and operational management. These are areas where computational modeling can provide insight and direction.

Atomistic techniques, including Density Functional Theory (DFT) and Molecular Dynamics (MD), and continuum techniques, including the Doyle−Fuller−Newman (DFN) model and its simplification, the single-particle model (SPM),[46,47] broadly describe battery modeling techniques from the atomic to the cell level.[48] DFT is well suited for investigating electronic structure, whereas MD, either *ab initio* or classical, can be used to provide vital information on system dynamics. These atomistic models can provide insights into material properties but can be limited by scale. Continuum modeling, a larger-scale computational technique, is better placed to provide cell-level properties. The DFN model assumes the electrodes are comprised of a homogeneous matrix of spherical particles and is able to predict the dynamics and internal states of a battery, for example, Li concentration within active materials. The SPM is a further simplification that considers one representative particle.

Combining atomistic and continuum model predictions within a multiscale modeling framework can provide a more detailed understanding of the charge and mass transport processes, resulting in more accurate predictions of battery behavior.[49−51] DFT has increasingly been utilized in parametrization of larger-scale techniques, such as classical MD.[50,52−56] One popular approach has been to use DFT calculations of migration mechanisms and activation barriers of Li-ions, in conjunction with classical MD studies of Li-ion diffusion, to gain a more complete analysis of the dynamic properties.[57,58] In a similar vein, DFT calculations of activation energies for different events are used to construct the basis for kinetic Monte Carlo (kMC) simulations.[59] kMC is a natural technique to include different time-scale dynamic events. For example, Röder et al. used a combination of the continuum-scale pseudo-two-dimensional (P2D) model and a heterogeneous surface film growth model based on kMC to obtain electrochemical information, including open-circuit potential (OCP), C-rate tests, and potential, during film formation.[60] These predictions were in good agreement with the equivalent experimental measurements.

In this Focus Review, drawing from our experience as part of the multiscale modeling project of the Faraday Institution in the United Kingdom, we highlight the importance of modeling NMC cathode materials across length and time scales. We also provide an outlook to current and future challenges faced in the modeling of multicomponent cathode materials for electrochemical energy storage.

Electrons: Oxidation-State Competition. The practical use of Ni-rich NMC materials in LIBs faces various challenges, including structural degradation and capacity fading. The redox reactions and consequent reversible capacity of NMCs are primarily influenced by the cation ordering and spin interaction of active elements in the transition-metal layers.[11,31,40,61,62] Different compositions and charge distributions result in the appearance of various charge states, e.g., Ni^{2+}, Ni^{3+}, Ni^{4+}, Co^{3+}, Co^{4+}, and Mn^{4+}.[62] The coexistence and interactions of these multivalent transition-metal charges and spins make it difficult to determine unique ground states for NMCs.[62] Understanding the range of transition-metal oxidation states, and the roles they play in degradation processes, is therefore crucial for improving these promising cathode materials.

Ni is a key redox-active element in NMCs. Experimentally, Ni in NMC811 is present as a mixture of Ni^{2+} (with ground-state electronic configuration of $t_{2g}^6e_g^2$) and $Ni^{3+}(t_{2g}^6e_g^2)$ oxidation states, with an average value close to 3+.[63−65] During charge−discharge cycling, Ni^{2+} can migrate from the Ni plane to the Li plane, creating Li/Ni disorder.[31,39,40] This leads to a structural transformation (layered to defective spinel/disordered rock-salt transition) and blocks the Li^+ migration channels.[40] Structural transformation is thought to be the origin of cracking and subsequent performance degradation upon lithium extraction.[37,64,66] The dissolution of NMCs, resulting in capacity attenuation, can occur due to metal disproportionation.[67] Ni disproportionation in pristine NMC811 has not been reported experimentally; however, simulations have predicted $2Ni^{3+} \rightarrow Ni^{2+} + Ni^{4+}$ disproportionation in $LiNiO_2$.[68] Charge disproportionation is observed in other cathode materials, such as pristine $LiMn_2O_4$, where $2Mn^{3+} \rightarrow Mn^{2+} + Mn^{4+}$ disproportionation is considered to be the main cause of Mn dissolution. Understanding active metal disproportionation is essential, as it poses a threat of poisoning the anode[69,70] and forming inorganic layers in solid electrolyte interphase (SEI) layers,[71] which, in turn, lead to capacity fade.

Understanding active metal disproportionation is essential, as it poses a threat of poisoning the anode.

The complex ordering and multivalent nature of transition metals pose significant challenges for modeling. Previous theoretical investigations have studied the influence of oxidation states on various properties of NMC materials.[25,72−76] These studies, employing various DFT functionals, have calculated Jahn−Teller distortion effects, atomic magnetic moments, and densities of states to assign metal oxidation states on the transition-metal atoms. There are discrepancies observed in the literature, depending on choice of method and functional used to calculate these properties.

Sun and Zhao[25] reported that Ni^{2+} is predominant over Ni^{3+} in NMC333, NMC442, and NMC532, whereas with the increase of Ni content, the occupation of Ni^{3+} steadily increases at the cost of Ni^{2+}, as shown in Figure 1a. In NMC811, the fraction of Ni^{3+} is reported as 58%, whereas there is no Ni^{4+} present in the pristine structure.[25] In contrast, Susai et al.[76] observed fractions of Ni^{2+}, Ni^{3+}, and Ni^{4+} at

https://doi.org/10.1021/acsenergylett.1c02028
ACS Energy Lett. 2022, 7, 108−122

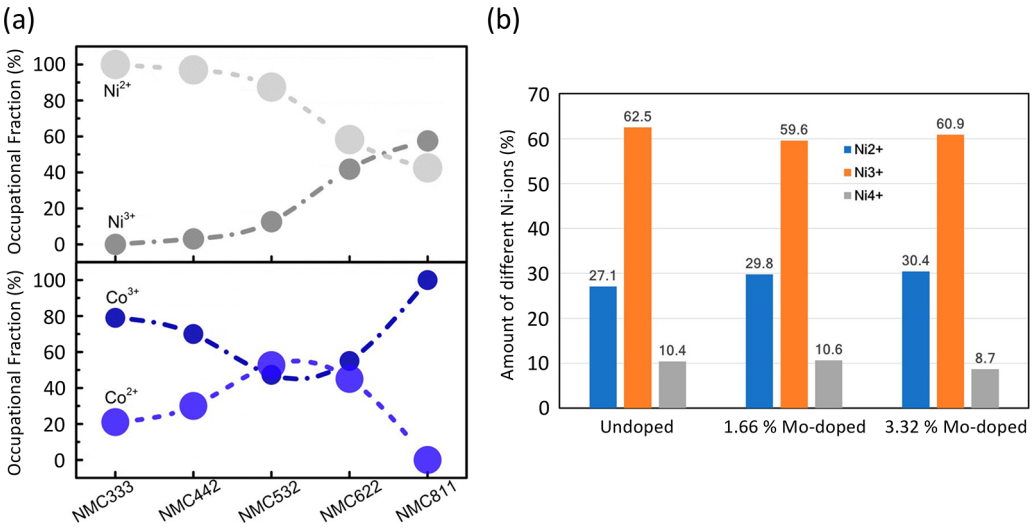

Figure 1. (a) Occupation fraction of Ni^{2+}/Ni^{3+} and Co^{2+}/Co^{3+} in five NMC compositions. Reprinted with permission from ref 25. Copyright 2017 American Chemical Society. (b) Distribution of Ni-ions in different oxidation states Ni^{2+}, Ni^{3+}, and Ni^{4+} for undoped and Mo-doped NMC811 materials. Adapted from ref 76.

around 27.1%, 62.5%, and 10.4%, respectively, as shown in Figure 1b. Dixit et al.[73] have also reported the presence of Ni^{4+} (~10%) along with Ni^{2+} (~23%) and Ni^{3+} (~66%), which is in closer agreement with the findings of Susai et al. The fraction of Ni^{4+} has been shown to be influenced by the lithiation state, with Ni^{4+} concentration increasing rapidly in Ni-rich NMC materials as a function of Li content. However, the distribution of Ni oxidation states is not greatly influenced by doping, Figure 1b.[73,76] Sun and Zhao[25] also reported on the existence of Co^{2+} ions along with Co^{3+} ions in pristine NMCs, an observation which was opposed by Dixit et al.[73] Based on magnetic moments and projected density of states calculations, Dixit et al. proposed that Co remains as Co^{3+} in different pristine NMCs.[73] Mn^{4+} remains in close proximity to Ni^{2+}, influencing the super-exchange interactions among transition metals.[77] The aforementioned discrepancies between methods could be associated with the different choice of functional, where Dixit et al.[73] employed a pure DFT approach. It could be also attributed to the use of different sets of effective "+U" on-site Coulomb interaction parameters for transition metals; e.g. the employed parameters vary as U_{eff} = 6.7, 4.2, and 4.91 eV,[25] and 5.96, 5.10, and 5.00 eV,[76] for Ni, Mn, and Co, respectively.

As mentioned earlier, specific transition-metal oxidation states have been implicated in degradation processes in NMC materials. With the mixed valence states of Ni^{2+}/Ni^{3+}, Ni^{3+} has the priority to exchange with Li and changes to a Ni^{2+} state with a spin-flip to form strong linear $Ni^{2+}-O_2-Ni^{2+}/Mn^{4+}$ super-exchange networks.[77,78] This acts as the driving force in tuning Ni/Li disorder. The presence of Ni^{4+} promotes electrolyte decomposition, forming side products that adversely affect Li^+ transport at the electrode−electrolyte interface, as well as thermal instability and oxygen evolution.[79] Therefore, proper elucidation of TM oxidation states in NMCs is required for their fruitful applications in LIBs. Although computationally demanding, to get better insight into the electronic properties of NMCs, the use of electronic structure approaches that can deal with the high levels of electron correlation and strong competition between oxidation states is necessary. Beyond DFT, the application of techniques such as dynamical mean field theory may yield important insights into complex transition-metal oxide electrodes.

Ions: Modeling of Diffusion. Understanding ion diffusion is crucial for the development of batteries with high power density, especially in solid electrodes, which present slow ion diffusion compared to electrolytes. Ionic diffusion can often be considered as a sequence of "hops" made by ions moving between distinct crystallographic sites.[80] The rate of diffusion can be understood through the diffusion coefficient, *D*.

Wei et al. used DFT to investigate the hopping mechanisms in a range of NMC compositions and lithiation states.[81] The authors found that Li is more likely to diffuse via oxygen dumbbell hopping (ODH) at the early stage of charging (delithiation). When more than one-third of the Li is removed, tetrahedral site hopping (TSH) becomes more dominant. For both ODH and TSH, Li surrounded by Ni is more likely to diffuse. Wei et al. also calculated diffusion coefficients for the same NMC compositions and found them to be several orders of magnitude larger than the experimental measurements.[81] Comparably, Cui et al. used DFT to calculate the diffusion coefficients of NMC532 and NMC622.[82] When compared to diffusion measured experimentally, the calculated DFT values were orders of magnitude larger than the experimental measurements. More recently, Zhu et al. also observed this disparity in the magnitude of the diffusion coefficients for NMC442, NMC532, NMC622, and NMC71515.[83] There have been several additional DFT studies on Li-ion migration in the pure bulk NMC-based materials using *ab initio* MD and nudged elastic band (NEB) techniques, most of which overestimate the diffusion rate in these materials, compared to experimental measurements of the real material.[84−88] DFT is well suited to investigating electronic properties and local hopping mechanisms.[87] However, when it comes to long-range diffusion, DFT is limited by time and length scales. Features which affect diffusion rates, such as grain boundaries and defects,[89] cannot be easily incorporated into the models. Classical MD is therefore better suited for calculating long-range diffusion, allowing simulations over longer time and length scales, and incorporating microstructural features not easily included at the DFT scale.

https://doi.org/10.1021/acsenergylett.1c02028
ACS Energy Lett. 2022, 7, 108−122

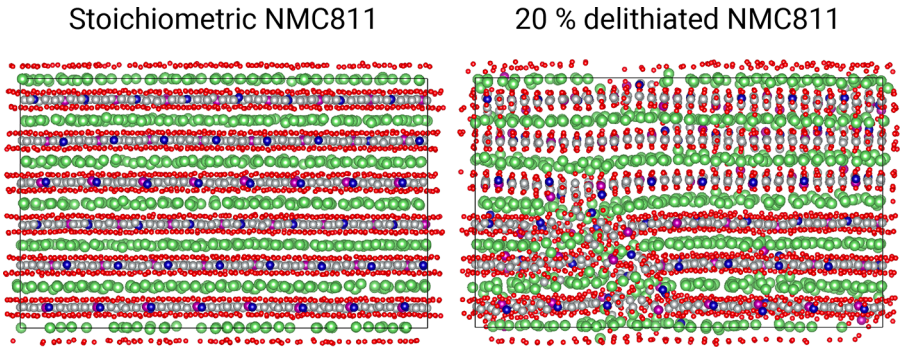

Figure 2. Structure images for fully lithiated and 20% delithiated NMC811 after an initial equilibration MD simulation using the interatomic potentials from Lee and Park.[107]

In classical MD, the chemical interactions are described using interatomic potentials.[90−93] There are many forms of interatomic potentials with the ability to describe heteropolar solids such as NMCs. A widely used interatomic potential for investigating diffusion properties is the Coulomb−Buckingham potential.[94] The Coulomb−Buckingham potential is derived from the Born model,[95,96] where the potential energy of the system is expressed as

$$E(r_{ij}) = \sum_{ij} \frac{Q_i Q_j}{4\pi\varepsilon_0 r_{ij}} + \sum_{ij} A \exp\left(\frac{-r_{ij}}{\rho}\right) - C r_{ij}^{-6} \quad (1)$$

Here, i and j are ions of charge Q_i and Q_j at a distance of r_{ij}, and ε_0 is the permittivity of free space. In the second term, A, ρ, and C are the parameters associated with the Buckingham potential. A describes long-range point charge electrostatic interactions, ρ is an exponentially decaying repulsive interaction that attempts to describe interatomic repulsion at short ion−ion separations, and C describes dispersion.

Core−shell models, such as the widely used adiabatic shell model,[97] can be used with interatomic potential to introduce polarizability into classical MD simulations.[98−102] This is done by separating the atom into two objects (the core and the shell) and tethering them together through a spring. The atomic mass is divided between the core and shell, commonly with 10% of the atomic mass assigned to the shell.[103,104] Standard rigid-ion models are not able to capture Jahn−Teller effects, which are known to be a pronounced feature in metal oxide materials such as NMCs.[21,25,72−76,105] By separating the core and shell into separate objects, through introducing a core−shell model, some aspect of the Jahn−Teller symmetry lowering can be described. However, a full treatment requires a description of angular overlap terms that require further parametrization.[106]

One classical MD study on NMCs, reported for NMC111, employed core−shell Buckingham potentials. Lee and Park investigated the defect energies in fully lithiated NMC111, finding the formation of defects to be unfavorable with high energies.[107] They found the most favorable defect formation as the Li−Ni anti-site defect (0.84 eV). The authors also attempted to analyze the Li^+ diffusion dynamics; however, with no Li vacancies present, hopping events would be infrequent and isolated. Therefore, migration was not observed within the 1 ns time frame.

To highlight the importance of capturing the complexities of layered oxide materials, such as mixed-metal charges, we used Lee and Park's potentials with different NMC compositions and states of lithiation. The charge placed on the Ni was adapted in accordance with the oxidation state in the composition as, to the best of our knowledge, no interatomic potentials exist in the literature for Ni^{3+}. We found that the potentials proposed for fully lithiated NMC111 are not transferable. Indeed, a catastrophic structural collapse is observed upon removing Li (Figure 2). Classical models based on fixed-charge modeling are incapable of describing dynamic redox processes and the associated Jahn−Teller instabilities. Different NMC compositions and lithiation states result in mixed transition-metal oxidation states and charge disproportion, as discussed previously. Representing this complexity with classical interatomic potential models is challenging.[108−110]

The development of interatomic potentials, which requires model parametrization with respect to a set of target observables, is a difficult task for these systems. For layered structures, variations of the Buckingham potential form have been developed, some using rigid-ion models,[111−114] and others using core−shell models,[99−102,107,111,115] with a mixture of formal and partial charges. We made attempts to apply the fitting routines from established codes, including the General Utility Lattice Program (GULP),[116] Atomicrex,[53] dftfit,[54] and potfit.[55] Each code possesses unique functionality; however, none was able to produce robust potentials, capable of adequately describing the atomic interactions, for NMCs or $LiNiO_2$. A software, POtential Parameter Optimisation for Force-Fields (PopOff),[52] has been specifically developed within the Faraday Institution for fitting different permutations of the Buckingham potential. Its modular design allows flexible fitting of both rigid-ion and core−shell models, as well as formal and partial charges. Here, we discuss important aspects of fitting cathode potentials using this code.

> If interatomic potentials are fit only to structural properties, they cannot be expected to describe the redox behavior of a cathode.

In systems such as NMCs and $LiNiO_2$, the longer-range Coulombic terms are much larger than the short-range interactions. In these cases, the atom charges need to be scaled down (partial charges) to restore the influence of the short-range interactions. A scaling factor of 60% formal charge is commonly used;[117] however, partial charges are system dependent. Figure 3a shows χ^2 (fit error) for a fitted Buckingham potential for $LiNiO_2$ reducing with the charge

https://doi.org/10.1021/acsenergylett.1c02028
ACS Energy Lett. 2022, 7, 108−122

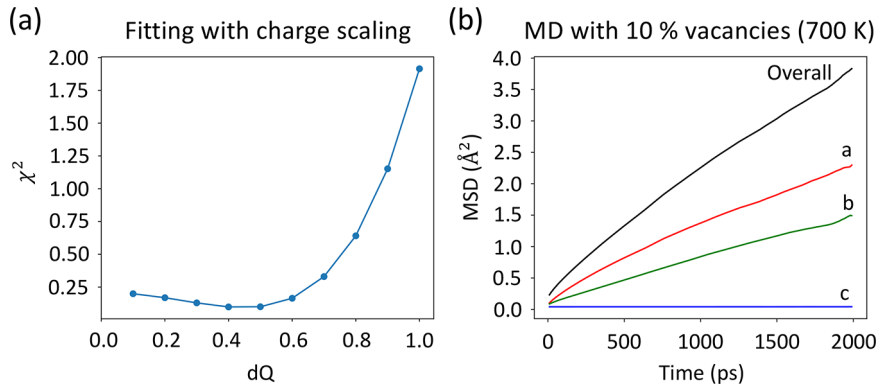

Figure 3. (a) Plot of the fit error, χ^2, of $LiNiO_2$ as a function of the charge scaling factor, d*Q*. (b) Plot of the mean-squared displacement of Li in $LiNiO_2$ with 10% Li vacancies at 700 K. As this is a layered material, it is expected that no movement will occur in the *c* direction, only in *a* and *b*.

scaling factor, until approximately 60% of the formal charge, where it starts to plateau. This is in broad agreement with literature, with a slightly improved fit at ∼50% formal charge.

Fitting rigid-ion potentials for $LiNiO_2$ with partial charges resulted in a fit error of $\chi^2 = 1.67$. By introducing a core−shell potential on the oxygen, with Li and Ni remaining rigid-ion, χ^2 was reduced to 0.37. This presents evidence that a core−shell potential is required to more accurately reproduce the forces and physics of the system. In the case of the oxygen core−shell potential, the fitting process resulted in a spring constant of 15.443 eV Å^{-2}, with a charge of −1.48 e on the shell and 0.520 e on the core. Here, the best fit (lowest χ^2) was a core−shell model on the oxygen in a partial charged system. The resulting potential was used with a 10% delithiated $LiNiO_2$ supercell at 700 K to conduct MD studies on the diffusion within the material. The mean-squared displacement, Figure 3b, represents small movements of Li; however, the resulting self-diffusion coefficient, 6.664×10^{-8} cm^2 s^{-1}, is within the measured range.[118,119] These results indicate that including a core−shell model for the oxygen and using partial charges are necessary to include in interatomic potential models, to get a more accurate representation of these systems.

The results presented here for comparing core−shell, rigid-ion, and formal/partial charges highlight the careful consideration needed when fitting potential models for heteropolar solids, such as NMCs. Fitting parameters also need to be tailored to the type of study being conducted. For example, if interatomic potentials are fit only to structural properties, they cannot be expected to describe the redox behavior of a cathode. If electronic features such as dielectric constant are included, then redox chemistry should be better represented. Other features such as charge equilibrium and ligand field effects should also be considered. Fitting to every material property is not feasible; however, fitting to a broad range of the properties most relevant to the study is needed.

Tools are currently in development to make fitting interatomic potentials more accessible, including more advanced statistical sampling that can train more robust models with less data.[52,53,55,120] In particular, machine learning (ML) has emerged as a powerful approach for developing interatomic potentials with more flexible functional forms.[56] One example is the development of accurate Li−Si potentials. Building on prior Si potentials,[121−123] Artrith et al. and Onat et al. both developed neural network models for Li in amorphous Si anodes.[124,125] These works helped underline the possibilities of ML potentials especially for battery materials modeling.[56] More generally, deep learning MD or "on-the-fly" ML is an emerging alternative for studying dynamic properties of materials beyond the limits of traditional simulations. Houchins and Viswanathan developed ML potentials for NMCs and used a neural network model, trained on DFT calculations with a prediction accuracy of 3.7 meV/atom and 0.13 eV/Å for energy and force, respectively.[126] Wang et al. also used ML interatomic potentials and MD coupled with on-the-fly ML tensor potentials.[127] The calculation efficiency was reported to increase by 7 orders of magnitude compared to *ab initio* MD, significantly reducing the uncertainty in calculated migration energies and improving agreement experiment. With all the proposed benefits of ML potentials, certain limitations should also be noted such as the treatment of long-range electrostatics that are critical for ionic solids. However, ongoing developments include the description of electrostatics model parameters, such as partial charges, local dipoles, and polarizability.[128,129]

Phonons: Thermal Transport. Crystals are often considered as consisting of atoms held in static positions through stiff chemical bonds. In reality, atoms are constantly vibrating around their average crystallographic positions in even the hardest of crystals. Lattice dynamics, based on the calculation of the interatomic force constants in a crystal, is a powerful tool to model thermal effects, from heat capacity to thermal expansion. Recently, the description of anharmonic effects including vibrational lifetimes and thermal conductivity has become accessible for multicomponent solids.

There have been a number of studies on the thermal properties of NMCs. Yang et al. reported the harmonic phonon dispersion for the $LiMO_2$ (M = Ni, Co, Mn) end points in the NMC oxide system.[105] These results reveal that the Jahn−Teller effect is more pronounced in the crystalline $LiMnO_2$, with three distinct bond lengths for the transition metal−O bonds. The authors found that the medium and low frequency modes are mainly due to motion of Li and transition metals, while the high frequency modes (>14 THz) are vibrations involving the transition metal and O atoms. The phonons also provide information on a group, where theoretical analysis within the group assigns the irreducible representations of the acoustic and optic branches. Of these, some modes are infrared (IR) active or Raman active, which is comparable with experimental IR/Raman spectra, with differences likely due to the volume expansion at finite temper-

https://doi.org/10.1021/acsenergylett.1c02028
ACS Energy Lett. 2022, 7, 108−122

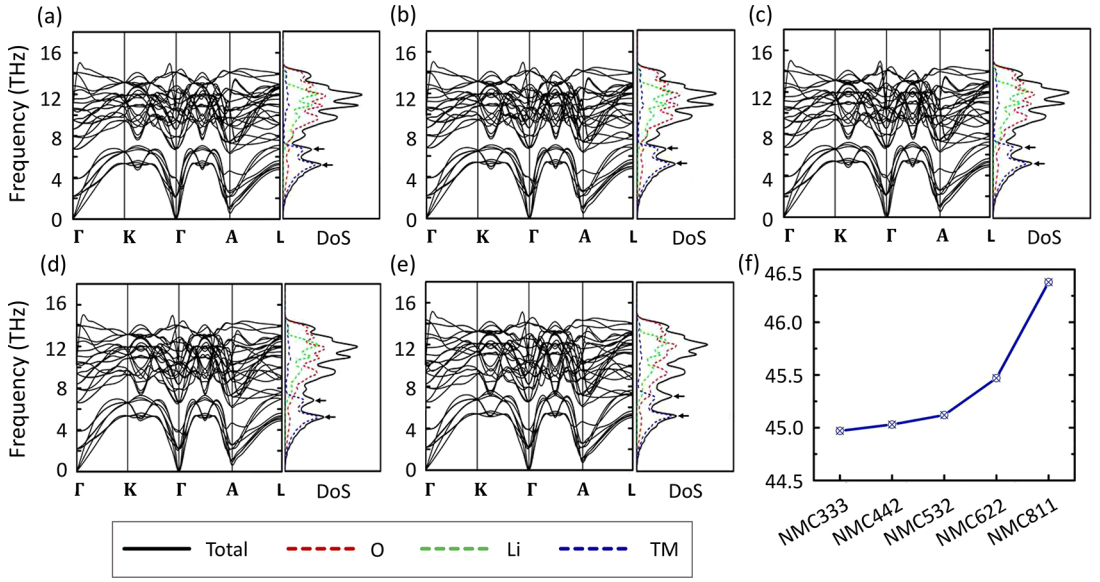

Figure 4. (a–e) Phonon dispersion and density of states (DoS) of NMC333, NMC442, NMC532, NMC622, and NMC811, respectively. Above the acoustic branch (0–6 THz) lies a dense optic phonon branch that reflects the structural complexity of these mixed-metal oxides. (f) Longitudinal acoustic frequency in the five NMC compounds around the Γ point of the Brillouin zone. Adapted from ref 25.

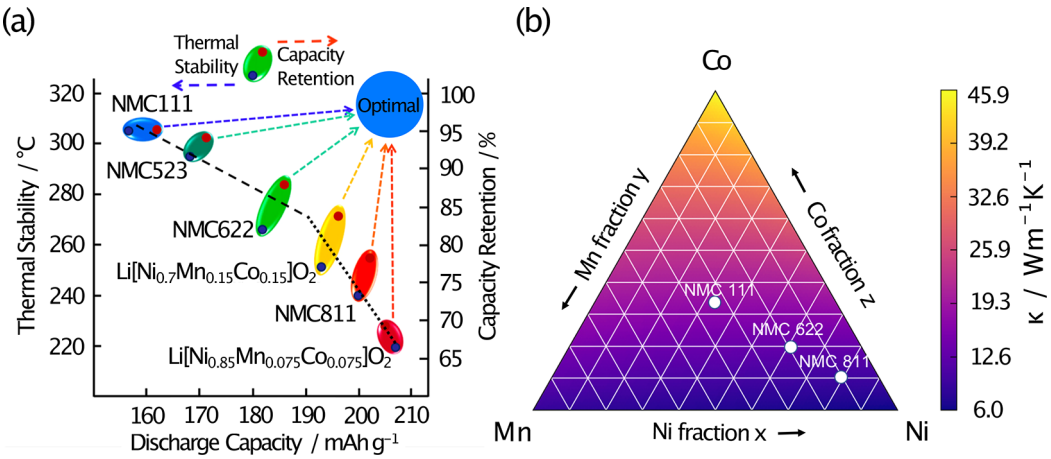

Figure 5. (a) Relation between discharge capacity, and thermal stability and capacity retention of NMC batteries. Adapted from ref 17. (b) Ternary map of the thermal conductivity map κ of the NMC system with consideration of mass variation at the cation site. Adapted from ref 105.

ature.[130] For NMC alloy systems, Sun and Zhao showed that the longitudinal acoustic mode frequency increases from NMC333 to NMC811 (Figure 4), due to the weaker electron screening.[25]

Both the electrochemical and thermal properties of NMCs depend on their composition. An increase in Ni content results in an increase in specific discharge capacity and total residual lithium content. However, the corresponding capacity retention and safety characteristics gradually decreased, as shown in Figure 5a.[17] Increasing Ni/Mn content leads to lattice thermal conductivity suppression.[105] Thermal conductivity decays exponentially with increasing temperature, due to enhanced phonon scattering, resulting from the larger thermal population of phonon modes. Figure 5b shows that, at room temperature, NMC811 has the lowest predicted thermal conductivity of 9.3 $W m^{-1} K^{-1}$, while NMC622 and NMC111 are higher at 13.3 and 17.9 $W m^{-1} K^{-1}$, respectively. In most devices, the thermal conductivity is much lower than these theoretical upper limits.[131,132] Both charging (delithiation) and having smaller grain sizes in polycrystalline cathode materials softens the lattice, leading to smaller phonon velocities and stronger phonon scattering.[133,134] These studies show the accessibility of tuning cathode material properties systematically by optimizing the ratio of the transition metals in NMC alloys, overcoming some of the challenges in battery cathode design.

Cells: Operation and Degradation. Atomistic modeling is ideal for investigating bulk and localized behavior; however, these predictions do not provide macroscopic information on material behavior at the cell level. Here, continuum models are well suited to provide further detail and insights. These are governed by mathematical expressions that relate concentrations and potentials (partial differential equations). Values describing different properties, such as diffusion coefficients and equilibrium potentials, are required as inputs or parameters, which can be obtained from experiments or using the atomistic simulation techniques discussed earlier.

https://doi.org/10.1021/acsenergylett.1c02028
ACS Energy Lett. 2022, 7, 108–122

Both the electrochemical and thermal properties of NMCs depend on their composition.

One example of a continuum-level model is the DFN model, this requires over 25 parameters, with the exact number being dependent on how the equations are expressed.[135] These parameters are related to the physical, chemical and electrochemical properties of the cell, incorporating the ionic and electron transport properties of individual electrodes and the electrolyte. Parameter estimation can be used to simplify the process, where only voltage and current measurements of the battery are used to elucidate the specific parameters, removing the need for a cell teardown, i.e., dismantling the cell to extract the components for extensive characterization.[136] Care must be taken due to the large number of parameters that have to be fitted, and the potential for over fitting. Computational expense can preclude the use of this model in battery management systems and often simple equivalent circuit models are favored instead.[137] The DFN model has been used extensively in battery material development, as it provides more detailed physical insights compared to other model classes.[138]

Recent interest in Ni-rich cathodes has seen the DFN model used extensively to understand the use of graded electrodes (containing multiple electrode particle sizes), to deconvolute capacity and power fade predictions, and to investigate the efficacy of tab and electrode designs for fast charging.[139−141] This research has been dependent on parameter sets for NMC materials being reported; however, these values may not reliably describe the properties of Ni-rich NMCs, because studies often use parameters determined for cathodes with lower/unknown Ni content. For example, Richardson et al. modeled an NMC material, using the properties of $LiNi_{0.4}Co_{0.6}O_2$, directly measured by Ecker et al.[139,142] Kindermann et al. measured the geometry of an NMC—with unknown stoichiometry—electrode, extracted from a Samsung cell.[140] Electrode diffusivity and reaction rates were estimated and not evaluated directly, while the equilibrium potential was represented by that of an NMC111 material reported elsewhere.[143]

Several NMC batteries with low nickel content have been experimentally parametrized.[142,144,145] Ecker et al. reporting of the physical and chemical properties of a commercial cell also offered a comparison of different techniques used to evaluate the electrode diffusivity.[142] Schmalstieg et al. investigated an NMC111 battery, mapping the exchange current density, its activation energy, and electrode diffusivity as a function of lithiation, by defining the stoichiometries of each electrode.[144] Liebig et al. studied the electrochemical behavior of a large format NMC cell, extending the model predictions to include thermal behavior.[145] These papers outline the cell properties required for simulations and the methods used to determine them. Thermal properties at the atomistic scale can be connected to performance and inform material selection for application. For example, $LiCoO_2$ has a significant entropy change compared to other cathode materials, including NMCs. Analysis for NMCs indicates a small amount of reversible heat generation, therefore thermal management of NMC-based batteries is more effective.[146] Parametrization is essential for modeling NMC cathode materials. Simulations act as a powerful tool to investigate the properties of NMCs and optimize design without the need to conduct resource-intensive experiments, but the reliability of predictions is dependent on the quality of data used to construct the model.[147]

Although the methodologies developed in these works can be applied to other materials, for modelers investigating Ni-rich NMC materials these properties provide limited utility, as they do not accurately describe their behavior.[148] This is attributed to the presence of different thermodynamic phases compared to NMC811, which affects the dependency of the material physical and electrochemical properties on the state of lithiation.[17] For example, the H2→H3 phase transition above 4.1 V has not been reported in NMC materials with Ni content below 80%.[149]

More recently, cells with NMC811 chemistries have been parametrized; Chen et al. elucidated the parameters for a commercial 21 700 cylindrical cell containing NMC811 vs graphite−SiO_x, and validated and tuning these values for cell discharge.[150] Sturm et al. reported a full electrochemical parametrization of a DFN model, to study lithium plating during fast charging of a NMC811/SiC cell.[141,151]

Traditionally, the sourcing of parameters required an extensive literature search and/or knowledge of prominent authors in the field, to collate a collection of parameters which represented the component parts in a cell. It should be noted that this often relied of various sources, with no complete data set from a single cell parametrization and validation experiment. Recently, the development of databases and software that collate parameter values for battery components have streamlined this process and proved essential for modeling applications.[152,153] Wang created a database that details over 100 parametrizations of batteries and the individual components and techniques that have been used to determine them.[154] Additionally, Python Battery Mathematical Modeling (PyBaMM), a software package explicitly developed for continuum modeling, caters for multiple model definitions (e.g., DFN, SPM, and SPMe (SPM with electrolyte)) and allows the construction of virtual batteries from various component chemistries.[155] These include parameters for the commercial NMC811 electrode mentioned above,[150] which have been utilized in multiple investigations.[152,153] PyBaMM is a powerful tool for in modeling NMC behavior, among other materials and cell chemistries. It provides researchers with

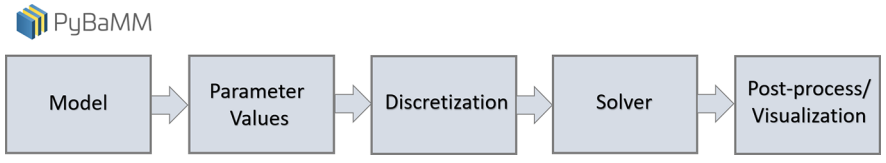

Figure 6. PyBaMM workflow has been designed to use a pipeline approach to define, discretize, and solve using electrochemical models. Adapted from ref 155.

https://doi.org/10.1021/acsenergylett.1c02028
ACS Energy Lett. 2022, 7, 108−122

parameter sets and robust code to simulate the electrochemical and thermal behavior in relatively few lines of code (Figure 6).

Validation of model predictions requires experimental data, from charge−discharge voltage curves at different current densities and long-term cycling experiments. Providing open data sets of parameter values and raw experimental validation data files improves accessibility and transparency of these models. There are several instances where data sets have been made available; Chen et al. have made available data on the discharge and subsequent relaxation of the NMC811-based cylindrical cell that was used in the validation of the parameter set in ref 156.[150] Devie et al. have provided data sets on the degradation of 18 650 cylindrical cells, based on NMC, NCA, and LFP chemistries.[157] This ongoing study examines the influence of operating conditions on the aging of cells (ref 158).

It is important to be aware of the nuances in reported parameter values which arise from the different test set-ups and methodologies, and the collation of values from various sources, some assumed or fitted, often used to populate the full parameter table. The thermal and electrochemical behaviors of battery materials have been widely described, being able to use these to accurately predict cell degradation has proven more difficult. Partially due to these difficulties in accurate parameter measurements during the cell cycling, and hence the limited full parameter and validation data sets from a single cell source. Edge et al. provide a detailed guide to understanding degradation modes, their mechanisms and the resulting effects, to design experiments and develop cell lifetime models.[159] There are two key degradation modes for the NMC positive electrode material which directly affect impedance, power, and capacity: loss of lithium inventory and loss of active material.[160,160] Repeated cycling causes volume changes, resulting in particle cracking,[161] and leading to loss of contact between the particles and current collector.[160] The cathode electrolyte interphase (CEI) layer, which forms in the cracks, triggers side reactions with the electrolyte, leading to passivation layer formation and consumption of lithium ions (LLI) and hence impedance increase.[160] Operating at high voltages (≥3.7 V) also promotes CEI formation, as well as other detrimental surface processes, such as gas evolution (O_2, CO_2, and CO).[162] NMC811 has a higher susceptibility toward oxygen evolution, due to its higher nickel content.[163] Long-term cycling and operating at high voltages and temperatures also causes dissolution of transition metals,[164] and NMC811 has a higher susceptibility to this due to the reactivity of highly oxidized nickel cations with the electrolyte.[165] Accurate prediction of cell behavior requires monitoring of these processes and deciphering of the interplay between processes. Knowledge of the changes in the physical, chemical and electrochemical parameters are needed for validation of these models. Examples of NMC degradation models include SPM[166,167] and DFN.[168]

Oxygen evolution can be modeled as the oxidation of electrolytes at the positive electrode introducing a simple, kinetically limited Tafel equation[166,168] in the DFN/SPM model. Jana et al. proposed that the capacity fade is a linear function of the oxidation current density, which the authors used in the Tafel equation to model the electrolyte oxidation at the NMC111-type positive electrode.[167] However, theoretical understanding and available models for the source of the oxygen evolution and its effect on the capacity fade are not well developed. Recently, Ghosh et al. have proposed a physics-based shrinking core model for the degradation of NMC811 electrodes that undergo a structural reorganization involving oxygen loss and the formation of a disordered (spinel or rock-salt structure) passivation layer.[169] The model considers O-release from the bulk−passivation layer interface, and the rate of reaction is controlled by either O-diffusion through the passivation layer or the reaction kinetics at the interface. Li entrapment and growth of the passivation layer cause capacity fade. Two limiting cases, "diffusion dominated" and "reaction dominated", manifest with a variation in the relative rates of O-diffusion and O-release, and the thickness of the passivation layer.

> Realistic models for cell lifetime and operation require a comprehensive understanding of degradation processes.

Transition-metal dissolution at the positive electrode is modeled using a first-order chemical reaction, limited by the concentration of H^+ ions in the electrolyte.[170] H^+ ions are generated from $LiPF_6$ salt dissociation in the electrolyte and solvent oxidation at the positive electrode. While $LiPF_6$ dissociation in the presence of H_2O is modeled using a chemical reaction rate, solvent oxidation is modeled using irreversible Butler−Volmer kinetics.[170] Lin et al. provide detailed DFN model equations for transition-metal dissolution at the lithium manganese oxide type positive electrode, coupled with SEI layer formation at the negative electrode. Transition-metal deposition on the negative electrode is also included in the model.[168] The growth of the CEI can be modeled in a similar way to any of the SEI layer growth models.

Key degradation processes that take place at the positive electrode material and their effects have been discussed, and fundamental characterization techniques that aide tracking and monitoring of these processes have been introduced. In order to use models to estimate aging mechanisms during normal or even fast charging, accurate determination of the parameters that describe the physical, chemical, and electrochemical properties of the cell is key. Electrochemical techniques are fast and practical diagnostic tools used in *in situ* characterization of battery performance, providing information on capacity, resistance, and Coulombic efficiency. The reliability of models to predict a cell's behavior is highly dependent on the type of cell and requires accurate experimental parameter and validation data, preferably from a single source cell.

SUMMARY AND OUTLOOK

We have reviewed recent progress in the modeling of NMC electrodes from the atomic scale to the cell scale. Looking at each length scale, a number of challenges can be identified. For electronic structure studies, proper elucidation of the oxidation states of mixed transition metals in NMC materials during battery cycling is important. Layered oxides with high Ni content have three critical challenges: cyclic degradation, thermal instability, and air instability, all of which are related to the reactivity of Ni^{3+} or Ni^{4+} in contact with the liquid organic electrolyte or ambient air.[43] The presence of multiple transition metals with mixed oxidation states also impacts the thermodynamic stability of NMC materials, which remain

https://doi.org/10.1021/acsenergylett.1c02028
ACS Energy Lett. 2022, 7, 108−122

difficult to describe in traditional phonon descriptions of crystal vibrations and associated free energy contributions.

For molecular dynamics studies, one bottleneck is the lack of interatomic potentials with the ability to accurately describe essential properties of electrodes, such as the redox chemistry associated with battery cycling. To achieve this, fitting potentials to better training data and more sophisticated functional forms is needed. Progress has also been made in using machine learning to develop more flexible potentials. Deringer et al. recently published a progress update, showing how machine learning is improving interatomic potentials by "learning" from electronic structure data, giving better accuracy in approximating material properties;[56] however, a challenge there is in the transfer from simple elemental solids to multicomponent oxides.

> Fitting potentials to better training data and more sophisticated functional forms is needed.

Inaccuracies in continuum models manifest due to the lack of complete parameter sets and differences in experimental design. Realistic models for cell lifetime and operation require a comprehensive understanding of degradation processes. To obtain representative data, greater physical and chemical characterization is needed, particularly from in situ studies. The use of multiple diagnostic tools can produce a rich data for greater accuracy in parametrization and validation of models, leading toward the design of more realistic models for lifetime prediction. It should also be noted that literature information may not be representative of the active material in the cell being modeled, and mistakes can easily be propagated.[48] The construction of a parameter database could prevent the reproduction of errors; however, equally important is an understanding of the experimental techniques used in parameter extraction and the model assumptions. Ideally, the theory underpinning the experimental parameter extraction needs to be consistent with that of the model to make truly robust predictions.

Lifetime predictions from continuum models do not necessarily need the precise degradation mechanism, as LAM or LLL can be reproduced through many different negative or positive electrode lithium loss mechanisms. However, greater understanding of the physics of the processes is required for truly accurate and predictive models. These can be used, for example, to identify key conditions for extending cell lifetime and performance. Degradation experiments and fundamental molecular-scale studies (including DFT), to understand the mechanisms, are essential for the development of whole-cell degradation models.[155]

Connecting continuum and atomistic model predictions can provide a more detailed understanding of the charge and mass transport processes, resulting in more powerful predictions of battery behavior. Attempts to join length scales have previously been attempted; however, there is no simple solution due to the difference in mathematical principles used in each model.[171] Continuum models comprise partial differential equations, while atomistic models often use discrete models.[172] This difference in mathematical principles leads to different calculable properties. For example, in atomistic modeling, charge transport is related to self-diffusion within the crystal, whereas charge transport in continuum modeling relates to macroscopic diffusion in the electrode, often being experimentally determined. Solutions to overcome this mismatch in calculable properties are of great interest and one of the biggest challenges in obtaining consistent, multiscale models of NMCs in particular and battery technologies in general.

AUTHOR INFORMATION

Corresponding Authors

Jacqueline Edge − *Department of Mechanical Engineering, Imperial College London, London SW7 2AZ, U.K.; The Faraday Institution, Didcot OX11 0RA, U.K.;* Email: j.edge@imperial.ac.uk

Aron Walsh − *Department of Materials, Imperial College London, London SW7 2AZ, U.K.; The Faraday Institution, Didcot OX11 0RA, U.K.; Department of Materials Science and Engineering, Yonsei University, Seoul 03722, Korea;* orcid.org/0000-0001-5460-7033; Email: a.walsh@imperial.ac.uk

Authors

Lucy M. Morgan − *Department of Chemistry, University of Bath, Bath BA2 7AY, U.K.; The Faraday Institution, Didcot OX11 0RA, U.K.*

Mazharul M. Islam − *Department of Chemistry, University of Bath, Bath BA2 7AY, U.K.; The Faraday Institution, Didcot OX11 0RA, U.K.*

Hui Yang − *Department of Materials, Imperial College London, London SW7 2AZ, U.K.; The Faraday Institution, Didcot OX11 0RA, U.K.;* orcid.org/0000-0002-7890-5411

Kieran O'Regan − *School of Metallurgy and Materials, University of Birmingham, Birmingham BT15 2TT, U.K.; The Faraday Institution, Didcot OX11 0RA, U.K.*

Anisha N. Patel − *Department of Mechanical Engineering, Imperial College London, London SW7 2AZ, U.K.; The Faraday Institution, Didcot OX11 0RA, U.K.;* orcid.org/0000-0002-4914-5062

Abir Ghosh − *Department of Mechanical Engineering, Imperial College London, London SW7 2AZ, U.K.; Department of Chemical Engineering & Technology, Indian Institute of Technology (BHU), Varanasi, Uttar Pradesh 221 005, India; The Faraday Institution, Didcot OX11 0RA, U.K.*

Emma Kendrick − *School of Metallurgy and Materials, University of Birmingham, Birmingham BT15 2TT, U.K.; The Faraday Institution, Didcot OX11 0RA, U.K.;* orcid.org/0000-0002-4219-964X

Monica Marinescu − *Department of Mechanical Engineering, Imperial College London, London SW7 2AZ, U.K.; The Faraday Institution, Didcot OX11 0RA, U.K.*

Gregory J. Offer − *Department of Mechanical Engineering, Imperial College London, London SW7 2AZ, U.K.; The Faraday Institution, Didcot OX11 0RA, U.K.*

Benjamin J. Morgan − *Department of Chemistry, University of Bath, Bath BA2 7AY, U.K.; The Faraday Institution, Didcot OX11 0RA, U.K.;* orcid.org/0000-0002-3056-8233

M. Saiful Islam − *Department of Chemistry, University of Bath, Bath BA2 7AY, U.K.; The Faraday Institution, Didcot OX11 0RA, U.K.;* orcid.org/0000-0003-3882-0285

Complete contact information is available at: https://pubs.acs.org/10.1021/acsenergylett.1c02028

https://doi.org/10.1021/acsenergylett.1c02028
ACS Energy Lett. 2022, 7, 108−122

Notes

The authors declare no competing financial interest.

Biographies

Lucy M. Morgan received her Ph.D. in chemistry from the University of Kent before taking a role as a postdoctoral research associate at the University of Bath. Her research has focused on scientific code development and the molecular dynamics modeling of NMC cathode materials and argyrodite solid electrolytes.

Mazharul M. Islam obtained his Ph.D. in theoretical chemistry from the University of Hannover and has since worked as a research associate/fellow at the University of South Australia, CNRS in Paris, the University of Bonn, and the University of Bath. He is currently a research associate at the University of Cardiff.

Hui Yang graduated with an Erasmus Mundus Masters in theoretical chemistry and computational modeling from KU Leuven (Belgium). She was awarded her Ph.D. in physics from University College London (UK) and is currently a postdoctoral researcher at the Imperial College London (UK), working on thermal transport in batteries.

Kieran O'Regan is a Ph.D. student at the University of Birmingham and the Faraday Institution. His research involves the parametrization of different battery chemistries, focusing on commercial cells. His research has led to the spin-off company About:Energy that provides tailored battery testing and modeling services to industry.

Anisha N. Patel received her Ph.D. from the University of Warwick in electrochemistry studying graphite. She completed a fellowship at the University of Paris Diderot, followed by a postdoc at Ulm University, and is currently a research electrochemist and facility manager focusing on failure in Li ion and solid-state batteries.

Abir Ghosh is an assistant professor at the Department of Chemical Engineering & Technology, IIT (BHU), Varanasi. He previously worked as a research associate at Imperial College London after finishing his Ph.D. at IIT Kanpur. His research focuses on thin film instability, microfluidics, electrochemical devices, and nanotechnology.

Emma Kendrick is a professor of energy materials at the University of Birmingham and has worked in industry and academia extensively on energy materials and devices. Her research focuses on the translation of novel functional materials into applications, with battery technology being a key theme. Emma holds over 100 publications and 21 patents.

Monica Marinescu is a senior lecturer in the Department of Mechanical Engineering at Imperial College. She creates a variety of models, electrochemical and reduced order, and bespoke experiments to identify the mechanisms limiting the performance of batteries and supercapacitors, and inform the design of better cells and packs.

Gregory J. Offer is a professor in electrochemical engineering, Imperial College London. His research is at the interface between the science and engineering of electrochemical devices and focuses on understanding the limits of operation, degradation mechanisms and failure modes of batteries, supercapacitors and fuel cells.

Benjamin J. Morgan is a Royal Society University Research Fellow at the University of Bath. His research uses atomic-scale modelling to understand energy materials, with a focus on understanding structure−composition−property relationships in lithium-ion battery materials.

M. Saiful Islam is professor of materials modeling at Oxford University after a period at the University of Bath. Raised in London, Saiful obtained his Ph.D. from UCL, followed by a fellowship at Eastman Kodak, New York. He received the 2020 ACS Award for Energy Chemistry and presented the 2016 BBC Royal Institution Christmas Lectures.

Jacqueline Edge completed her Ph.D. in hydrogen storage at UCL and then ran the Energy Storage Research Network in the Energy Futures Lab at Imperial College London. She currently works in the Mechanical Engineering Department as a project leader for the Faraday Institution, managing the Multiscale Modelling of Li-ion Batteries project.

Aron Walsh is a professor of materials design at Imperial College London. He leads a team of researchers working on the development and application of computational tools to model energy conversion and transport in materials at the atomic scale.

■ ACKNOWLEDGMENTS

The authors thank the Faraday Institution (https://faraday.ac.uk/; EP/S003053/1), grant number FIRG003, for funding.

■ REFERENCES

(1) Whittingham, M. S. The hydrated intercalation complexes of the layered disulfides. *Mater. Res. Bull.* **1974**, *9*, 1681−1689.
(2) Whittingham, M. S. Electrical energy storage and intercalation chemistry. *Science* **1976**, *192*, 1126−1127.
(3) Mizushima, K.; Jones, P.; Wiseman, P.; Goodenough, J. B. Li_xCoO_2 ($0 < x < -1$): A new cathode material for batteries of high energy density. *Mater. Res. Bull.* **1980**, *15*, 783−789.
(4) Armand, M.; Tarascon, J.-M. Building better batteries. *Nature* **2008**, *451*, 652−657.
(5) Scrosati, B.; Hassoun, J.; Sun, Y.-K. Lithium-ion batteries. A look into the future. *Energy Environ. Sci.* **2011**, *4*, 3287−3295.
(6) Goodenough, J. B.; Park, K.-S. The Li-Ion Rechargeable Battery: A Perspective. *J. Am. Chem. Soc.* **2013**, *135*, 1167−1176.
(7) Etacheri, V.; Marom, R.; Elazari, R.; Salitra, G.; Aurbach, D. Challenges in the development of advanced Li-ion batteries: a review. *Energy Environ. Sci.* **2011**, *4*, 3243−3262.
(8) He, P.; Yu, H.; Zhou, H.; et al. Layered lithium transition metal oxide cathodes towards high energy lithium-ion batteries. *J. Mater. Chem.* **2012**, *22*, 3680−3695.
(9) Rozier, P.; Tarascon, J. M. Review-Li-Rich Layered Oxide Cathodes for Next-Generation Li-Ion Batteries: Chances and Challenges. *J. Electrochem. Soc.* **2015**, *162*, A2490−A2499.
(10) Dunn, B.; Kamath, H.; Tarascon, J.-M. Electrical energy storage for the grid: a battery of choices. *Science* **2011**, *334*, 928−935.
(11) Maleki Kheimeh Sari, H.; Li, X. Controllable Cathode−Electrolyte Interface of $Li[Ni_{0.8}Co_{0.1}Mn_{0.1}]O_2$ for Lithium Ion Batteries: A Review. *Adv. Energy Mater.* **2019**, *9*, 1901597.
(12) Julien, C. M.; Mauger, A.; Zaghib, K.; Groult, H. Comparative issues of cathode materials for Li-ion batteries. *Inorganics* **2014**, *2*, 132−154.
(13) Whittingham, M. S. Materials challenges facing electrical energy storage. *MRS Bull.* **2008**, *33*, 411−419.
(14) Bruce, P. G.; Freunberger, S. A.; Hardwick, L. J.; Tarascon, J.-M. $Li−O_2$ and Li−S batteries with high energy storage. *Nat. Mater.* **2012**, *11*, 19.
(15) Gibbard, H. High Temp., High Pulse Power Lithium Batteries. *J. Power Sources* **1989**, *26*, 81−91.
(16) Plichta, E.; Slane, S.; Uchiyama, M.; Salomon, M.; Chua, D.; Ebner, W.; Lin, H. An Improved Li/Li_xCoO_2 Rechargeable Cell. *J. Electrochem. Soc.* **1989**, *136*, 1865−1869.
(17) Noh, H.-J.; Youn, S.; Yoon, C. S.; Sun, Y.-K. Comparison of the structural and electrochemical properties of layered $Li[Ni_xCo_yMn_z]O_2$ (x= 1/3, 0.5, 0.6, 0.7, 0.8 and 0.85) cathode material for lithium-ion batteries. *J. Power Sources* **2013**, *233*, 121−130.
(18) Mo, J.; Jeon, W. The Impact of Electric Vehicle Demand and Battery Recycling on Price Dynamics of Lithium-Ion Battery Cathode

https://doi.org/10.1021/acsenergylett.1c02028
ACS Energy Lett. 2022, 7, 108−122

Materials: A Vector Error Correction Model (VECM) Analysis. *Sustainability* **2018**, *10*, 2870.
(19) Banza, C. L. N.; Nawrot, T. S.; Haufroid, V.; Decrée, S.; De Putter, T.; Smolders, E.; Kabyla, B. I.; Luboya, O. N.; Ilunga, A. N.; Mutombo, A. M.; Nemery, B. High human exposure to cobalt and other metals in Katanga, a mining area of the Democratic Republic of Congo. *Environ. Res.* **2009**, *109*, 745−752.
(20) Min, K.; Kim, K.; Jung, C.; Seo, S.-W.; Song, Y. Y.; Lee, H. S.; Shin, J.; Cho, E. A comparative study of structural changes in lithium nickel cobalt manganese oxide as a function of Ni content during delithiation process. *J. Power Sources* **2016**, *315*, 111−119.
(21) Tian, Z.; Yu, H.; Zhang, Z.; Xu, X. Performance Improvements of Cobalt Oxide Cathodes for Rechargeable Lithium Batteries. *ChemBioEng Rev.* **2018**, *5*, 111−118.
(22) Paulsen, J.; Thomas, C.; Dahn, J. O_2 Structure $Li_{2/3}[Ni_{1/3}Mn_{2/3}]O_2$: A New Layered Cathode Material for Rechargeable Lithium Batteries. I. Electrochemical Properties. *J. Electrochem. Soc.* **2000**, *147*, 861.
(23) Paulsen, J.; Dahn, J. O_2-Type $Li_{2/3}[Ni_{1/3}Mn_{2/3}]O_2$: A New Layered Cathode Material for Rechargeable Lithium Batteries II. Structure, Composition, and Properties. *J. Electrochem. Soc.* **2000**, *147*, 2478.
(24) Lu, Z.; MacNeil, D.; Dahn, J. Layered cathode materials $Li[Ni_xLi_{(1/3-2x/3)}Mn_{(2/3-x/3)}]O_2$ for lithium-ion batteries. *Electrochem. Solid-State Lett.* **2001**, *4*, A191.
(25) Sun, H.; Zhao, K. Electronic Structure and Comparative Properties of $LiNi_xMn_yCo_zO_2$ Cathode Materials. *J. Phys. Chem. C* **2017**, *121*, 6002−6010.
(26) Larcher, D.; Tarascon, J.-M. Towards greener and more sustainable batteries for electrical energy storage. *Nat. Chem.* **2015**, *7*, 19.
(27) Ohzuku, T.; Makimura, Y. Layered lithium insertion material of $LiCo_{1/3}Ni_{1/3}Mn_{1/3}O_2$ for lithium-ion batteries. *Chem. Lett.* **2001**, *30*, 642−643.
(28) Dahn, J.; Von Sacken, U.; Juzkow, M.; Al-Janaby, H. Rechargeable $LiNiO_2$/carbon cells. *J. Electrochem. Soc.* **1991**, *138*, 2207−2211.
(29) Kim, M.-H.; Shin, H.-S.; Shin, D.; Sun, Y.-K. Synthesis and electrochemical properties of $Li[Ni_{0.8}Co_{0.1}Mn_{0.1}]O_2$ and $Li[Ni_{0.8}Co_{0.2}]O_2$ via co-precipitation. *J. Power Sources* **2006**, *159*, 1328−1333.
(30) Armstrong, A. R.; Bruce, P. G. Synthesis of layered $LiMnO_2$ as an electrode for rechargeable lithium batteries. *Nature* **1996**, *381*, 499.
(31) Duan, Y.; Yang, L.; Zhang, M.-J.; Chen, Z.; Bai, J.; Amine, K.; Pan, F.; Wang, F. Insights into Li/Ni ordering and surface reconstruction during synthesis of Ni-rich layered oxides. *J. Mater. Chem. A* **2019**, *7*, 513−519.
(32) Zhang, N.; Li, J.; Li, H.; Liu, A.; Huang, Q.; Ma, L.; Li, Y.; Dahn, J. R. Structural, Electrochemical, and Thermal Properties of Nickel-Rich $LiNi_xMn_yCo_zO_2$ Materials. *Chem. Mater.* **2018**, *30*, 8852−8860.
(33) Azevedo, M.; Campagnol, N.; Hagenbruch, T.; Hoffman, K.; Lala, A.; Ramsbottom, O. Lithium and cobalt: A tale of two commodities, Jun 22, 2018;https://www.mckinsey.com/industries/metals-and-mining/our-insights/lithium-and-cobalt-a-tale-of-two-commodities (accessed 01-11-2021).
(34) Myung, S.-T.; Maglia, F.; Park, K.-J.; Yoon, C. S.; Lamp, P.; Kim, S.-J.; Sun, Y.-K. Nickel-Rich Layered Cathode Materials for Automotive Lithium-Ion Batteries: Achievements and Perspectives. *ACS Energy Letters* **2017**, *2*, 196−223.
(35) Belharouak, I.; Sun, Y.-K.; Liu, J.; Amine, K. $Li(Ni_{1/3}Co_{1/3}Mn_{1/3})O_2$ as a suitable cathode for high power applications. *J. Power Sources* **2003**, *123*, 247−252.
(36) Kim, J. W.; Travis, J. J.; Hu, E.; Nam, K.-W.; Kim, S. C.; Kang, C. S.; Woo, J.-H.; Yang, X.-Q.; George, S. M.; Oh, K. H.; et al. Unexpected high power performance of atomic layer deposition coated $Li[Ni_{1/3}Mn_{1/3}Co_{1/3}]O_2$ cathodes. *J. Power Sources* **2014**, *254*, 190−197.
(37) Li, J.; Manthiram, A. A Comprehensive Analysis of the Interphasial and Structural Evolution over Long-Term Cycling of Ultrahigh-Nickel Cathodes in Lithium-Ion Batteries. *Adv. Energy Mater.* **2019**, *9*, 1902731.
(38) Jerng, S. E.; Chang, B.; Shin, H.; Kim, H.; Lee, T.; Char, K.; Choi, J. W. Pyrazine-Linked 2D Covalent Organic Frameworks as Coating Material for High-Nickel Layered Oxide Cathodes in Lithium-Ion Batteries. *ACS Appl. Mater. Interfaces* **2020**, *12*, 10597−10606.
(39) Zhang, S.; Ma, J.; Hu, Z.; Cui, G.; Chen, L. Identifying and addressing critical challenges of high-voltage layered ternary oxide cathode materials. *Chem. Mater.* **2019**, *31*, 6033−6065.
(40) Xia, Y.; Zheng, J.; Wang, C.; Gu, M. Designing principle for Ni-rich cathode materials with high energy density for practical applications. *Nano Energy* **2018**, *49*, 434−452.
(41) De Biasi, L.; Schwarz, B.; Brezesinski, T.; Hartmann, P.; Janek, J.; Ehrenberg, H. Chemical, Structural, and Electronic Aspects of Formation and Degradation Behavior on Different Length Scales of Ni-Rich NCM and Li-Rich HE-NCM Cathode Materials in Li-Ion Batteries. *Adv. Mater.* **2019**, *31*, 1900985.
(42) Li, W.; Dolocan, A.; Oh, P.; Celio, H.; Park, S.; Cho, J.; Manthiram, A. Dynamic behaviour of interphases and its implication on high-energy-density cathode materials in lithium-ion batteries. *Nat. Commun.* **2017**, *8*, 14589.
(43) Manthiram, A. A reflection on lithium-ion battery cathode chemistry. *Nat. Commun.* **2020**, *11*, 1550.
(44) Vetter, J.; Novák, P.; Wagner, M. R.; Veit, C.; Möller, K.-C.; Besenhard, J.; Winter, M.; Wohlfahrt-Mehrens, M.; Vogler, C.; Hammouche, A. Ageing mechanisms in lithium-ion batteries. *J. Power Sources* **2005**, *147*, 269−281.
(45) Liu, J.; Zou, Z.; Zhang, S.; Zhang, H. Structure, modification, and commercialization of high nickel ternary material ($LiNi_{0.8}Co_{0.1}Mn_{0.1}O_2$ and $LiNi_{0.8}Co_{0.15}Al_{0.05}O_2$) for lithium ion batteries. *J. Solid State Electrochem.* **2021**, *25*, 387−410.
(46) Newman, J.; Tiedemann, W. Porous-electrode theory with battery applications. *AIChE J.* **1975**, *21*, 25−41.
(47) Doyle, M.; Fuller, T.; Newman, J. Modeling of Galvanostatic Charge and Discharge of the Lithium/Polymer/Insertion Cell. *J. Electrochem. Soc.* **1993**, *140*, 1526.
(48) Howey, D. A.; Roberts, S. A.; Viswanathan, V.; Mistry, A.; Beuse, M.; Khoo, E.; DeCaluwe, S. C. Free Radicals: Making a Case for Battery Modeling. *Electrochemical Society Interface* **2020**, *29*, 30−34.
(49) Franco, A. A. Multiscale modelling and numerical simulation of rechargeable lithium ion batteries: concepts, methods and challenges. *RSC Adv.* **2013**, *3*, 13027−13058.
(50) Franco, A. A.; Rucci, A.; Brandell, D.; Frayret, C.; Gaberscek, M.; Jankowski, P.; Johansson, P. Boosting Rechargeable Batteries R&D by Multiscale Modeling: Myth or Reality? *Chem. Rev.* **2019**, *119*, 4569−4627.
(51) Shi, S.; Gao, J.; Liu, Y.; Zhao, Y.; Wu, Q.; Ju, W.; Ouyang, C.; Xiao, R. Multi-scale computation methods: Their applications in lithium-ion battery research and development. *Chin. Phys. B* **2016**, *25*, 018212.
(52) Morgan, L. M.; Clarke, M.; Islam, M. S.; Morgan, B. J. *PopOff: POtential Parameter Optimisation for Force-Fields*, 2021; DOI: 10.5281/zenodo.4773795.
(53) Stukowski, A.; Fransson, E.; Mock, M.; Erhart, P. Atomicrex−a general purpose tool for the construction of atomic interaction models. *Modell. Simul. Mater. Sci. Eng.* **2017**, *25*, 055003.
(54) Ostrouchov, C. dftfit; https://chrisostrouchov.com/dftfit.
(55) Wen, M.; Li, J.; Brommer, P.; Elliott, R. S.; Sethna, J. P.; Tadmor, E. B. A KIM-compliant *potfit* for fitting sloppy interatomic potentials: application to the EDIP model for silicon. *Modell. Simul. Mater. Sci. Eng.* **2017**, *25*, 014001.
(56) Deringer, V. L.; Caro, M. A.; Csányi, G. Machine learning interatomic potentials as emerging tools for materials science. *Adv. Mater.* **2019**, *31*, 1902765.

(57) Vicent-Luna, J. M.; Ortiz-Roldan, J. M.; Hamad, S.; Tena-Zaera, R.; Calero, S.; Anta, J. A. Quantum and classical molecular dynamics of ionic liquid electrolytes for Na/Li-based batteries: molecular origins of the conductivity behavior. *ChemPhysChem* **2016**, *17*, 2473−2481.
(58) Choi, Y.-S.; Park, J.-H.; Ahn, J.-P.; Lee, J.-C. Interfacial reactions in the Li/Si diffusion couples: origin of anisotropic lithiation of crystalline Si in Li−Si batteries. *Sci. Rep.* **2017**, *7*, 14028.
(59) Gavilán-Arriazu, E. M.; Mercer, M. P.; Barraco, D. E.; Hoster, H. E.; Leiva, E. P. M. Kinetic Monte Carlo simulations applied to Li-ion and post Li-ion batteries: a key link in the multi-scale chain. *Progress in Energy* **2021**, *3*, 042001.
(60) Röder, F.; Laue, V.; Krewer, U. Model Based Multiscale Analysis of Film Formation in Lithium-Ion Batteries. *Batteries & Supercaps* **2019**, *2*, 248−265.
(61) Li, G.; Liao, Y.; Li, Z.; Xu, N.; Lu, Y.; Lan, G.; Sun, G.; Li, W. Constructing a Low-Impedance Interface on a High-Voltage $LiNi_{0.8}Co_{0.1}Mn_{0.1}O_2$ Cathode with 2, 4, 6-Triphenyl Boroxine as a Film-Forming Electrolyte Additive for Li-Ion Batteries. *ACS Appl. Mater. Interfaces* **2020**, *12*, 37013−37026.
(62) Xiao, Y.; et al. Insight into the origin of lithium/nickel ions exchange in layered $Li(Ni_xMn_yCo_z)O_2$ cathode materials. *Nano Energy* **2018**, *49*, 77−85.
(63) Zhu, J.; Chen, G. Single-crystal based studies for correlating the properties and high-voltage performance of $Li[Ni_xMn_yCo_{1-x-y}]O_2$ cathodes. *J. Mater. Chem. A* **2019**, *7*, 5463−5474.
(64) M arker, K.; Reeves, P. J.; Xu, C.; Griffith, K. J.; Grey, C. P. Evolution of Structure and Lithium Dynamics in $LiNi_{0.8}Mn_{0.1}Co_{0.1}O_2$ (NMC811) Cathodes during Electrochemical Cycling. *Chem. Mater.* **2019**, *31*, 2545−2554.
(65) Kondrakov, A. O.; Geßwein, H.; Galdina, K.; de Biasi, L.; Meded, V.; Filatova, E. O.; Schumacher, G.; Wenzel, W.; Hartmann, P.; Brezesinski, T.; Janek, J. Charge-Transfer-Induced Lattice Collapse in Ni-Rich NCM Cathode Materials during Delithiation. *J. Phys. Chem. C* **2017**, *121*, 24381−24388.
(66) Li, T.; Yuan, X.-Z.; Zhang, L.; Song, D.; Shi, K.; Bock, C. Degradation Mechanisms and Mitigation Strategies of Nickel-Rich NMC-Based Lithium-Ion Batteries. *Electrochemical Energy Reviews* **2020**, *3*, 43−80.
(67) Buchberger, I.; Seidlmayer, S.; Pokharel, A.; Piana, M.; Hattendorff, J.; Kudejova, P.; Gilles, R.; Gasteiger, H. A. Aging analysis of graphite/$LiNi_{1/3}Mn_{1/3}Co_{1/3}O_2$ cells using XRD, PGAA, and AC impedance. *J. Electrochem. Soc.* **2015**, *162*, A2737.
(68) Chen, H.; Freeman, C. L.; Harding, J. H. Charge disproportionation and Jahn-Teller distortion in $LiNiO_2$ and $NaNiO_2$: A density functional theory study. *Phys. Rev. B: Condens. Matter Mater. Phys.* **2011**, *84*, 085108.
(69) Parmar, R.; Rezvani, S.; Nobili, F.; Di Cicco, A.; Trapananti, A.; Minicucci, M.; Nannarone, S.; Giglia, A.; Maroni, F.; Gunnella, R. Electrochemical Response and Structural Stability of the Li^+ Ion Battery Cathode with Coated $LiMn_2O_4$ Nanoparticles. *ACS Applied Energy Materials* **2020**, *3*, 8356−8365.
(70) Pasqualini, M.; Calcaterra, S.; Maroni, F.; Rezvani, S.; Di Cicco, A.; Alexander, S.; Rajantie, H.; Tossici, R.; Nobili, F. Electrochemical and spectroscopic characterization of an alumina-coated LiMn2O4 cathode with enhanced interfacial stability. *Electrochim. Acta* **2017**, *258*, 175−181.
(71) Joshi, T.; Eom, K.; Yushin, G.; Fuller, T. F. Effects of dissolved transition metals on the electrochemical performance and SEI growth in lithium-ion batteries. *J. Electrochem. Soc.* **2014**, *161*, A1915.
(72) Chakraborty, A.; Kunnikuruvan, S.; Kumar, S.; Markovsky, B.; Aurbach, D.; Dixit, M.; Major, D. T. Layered Cathode Materials for Lithium-Ion Batteries: Review of Computational Studies on $LiNi_{1-x-y}Co_xMn_yO_2$ and $LiNi_{1-x-y}Co_xAl_yO_2$. *Chem. Mater.* **2020**, *32*, 915−952.
(73) Dixit, M.; Markovsky, B.; Schipper, F.; Aurbach, D.; Major, D. T. Origin of Structural Degradation During Cycling and Low Thermal Stability of Ni-Rich Layered Transition Metal-Based Electrode Materials. *J. Phys. Chem. C* **2017**, *121*, 22628−22636.
(74) Hoang, K.; Johannes, M. Defect Physics and Chemistry in Layered Mixed Transition Metal Oxide Cathode Materials: (Ni,Co,Mn) vs (Ni,Co,Al). *Chem. Mater.* **2016**, *28*, 1325−1334.
(75) Dixit, M.; Markovsky, B.; Aurbach, D.; Major, D. T. Unraveling the Effects of Al Doping on the Electrochemical Properties of $LiNi_{0.5}Co_{0.2}Mn_{0.3}O_2$ Using First Principles. *J. Electrochem. Soc.* **2017**, *164*, A6359−A6365.
(76) Susai, F. A.; Kovacheva, D.; Chakraborty, A.; Kravchuk, T.; Ravikumar, R.; Talianker, M.; Grinblat, J.; Burstein, L.; Kauffmann, Y.; Major, D. T.; et al. Improving performance of $LiNi_{0.8}Co_{0.1}Mn_{0.1}O_2$ cathode materials for lithium-ion batteries by doping with molybdenum-ions: theoretical and experimental studies. *ACS applied energy materials* **2019**, *2*, 4521−4534.
(77) Zheng, J.; Ye, Y.; Liu, T.; Xiao, Y.; Wang, C.; Wang, F.; Pan, F. Ni/Li disordering in layered transition metal oxide: electrochemical impact, origin, and control. *Acc. Chem. Res.* **2019**, *52*, 2201−2209.
(78) Zheng, J.; Teng, G.; Xin, C.; Zhuo, Z.; Liu, J.; Li, Q.; Hu, Z.; Xu, M.; Yan, S.; Yang, W.; et al. Role of Superexchange Interaction on Tuning of Ni/Li Disordering in Layered Li $(Ni_xMn_yCo_z)O_2$. *J. Phys. Chem. Lett.* **2017**, *8*, 5537−5542.
(79) Bak, S.-M.; Hu, E.; Zhou, Y.; Yu, X.; Senanayake, S. D.; Cho, S.-J.; Kim, K.-B.; Chung, K. Y.; Yang, X.-Q.; Nam, K.-W. Structural changes and thermal stability of charged $LiNi_xM_yCo_zO_2$ cathode materials studied by combined in situ time-resolved XRD and mass spectroscopy. *ACS Appl. Mater. Interfaces* **2014**, *6*, 22594−22601.
(80) Catlow, C. R. A. Static lattice simulation of structure and transport in superionic conductors. *Solid State Ionics* **1983**, *8*, 89−107.
(81) Wei, Y.; Zheng, J.; Cui, S.; Song, X.; Su, Y.; Deng, W.; Wu, Z.; Wang, X.; Wang, W.; Rao, M.; et al. Kinetics tuning of Li-ion diffusion in layered $Li(Ni_xMn_yCo_z)O_2$. *J. Am. Chem. Soc.* **2015**, *137*, 8364−8367.
(82) Cui, S.; Wei, Y.; Liu, T.; Deng, W.; Hu, Z.; Su, Y.; Li, H.; Li, M.; Guo, H.; Duan, Y.; et al. Optimized temperature effect of li-ion diffusion with layer distance in $Li(Ni_xMn_yCo_z)O_2$ cathode materials for high performance Li-ion battery. *Adv. Energy Mater.* **2016**, *6*, 1501309.
(83) Zhu, Y.; Huang, Y.; Du, R.; Tang, M.; Wang, B.; Zhang, J. Effect of Ni^{2+} on Lithium-Ion Diffusion in Layered $Li-Ni_{1-x-y}Mn_xCo_yO_2$ Materials. *Crystals* **2021**, *11*, 465.
(84) Dixit, M.; Kosa, M.; Lavi, O. S.; Markovsky, B.; Aurbach, D.; Major, D. T. Thermodynamic and kinetic studies of $Li-Ni_{0.5}Co_{0.2}Mn_{0.3}O_2$ as a positive electrode material for Li-ion batteries using first principles. *Phys. Chem. Chem. Phys.* **2016**, *18*, 6799−6812.
(85) Huang, Z.; Wang, Z.; Jing, Q.; Guo, H.; Li, X.; Yang, Z. Investigation on the effect of Na doping on structure and Li-ion kinetics of layered $LiNi_{0.6}Co_{0.2}Mn_{0.2}O_2$ cathode material. *Electrochim. Acta* **2016**, *192*, 120−126.
(86) Li, S.; Yao, Z.; Zheng, J.; Fu, M.; Cen, J.; Hwang, S.; Jin, H.; Orlov, A.; Gu, L.; Wang, S.; et al. Direct Observation of Defect-Aided Structural Evolution in a Nickel-Rich Layered Cathode. *Angew. Chem.* **2020**, *132*, 22276−22283.
(87) Van der Ven, A.; Ceder, G. Lithium diffusion mechanisms in layered intercalation compounds. *J. Power Sources* **2001**, *97*−*98*, 529−531.
(88) Xiao, R.; Li, H.; Chen, L. Density functional investigation on Li_2MnO_3. *Chem. Mater.* **2012**, *24*, 4242−4251.
(89) Abakumov, A. M.; Li, C.; Boev, A.; Aksyonov, D. A.; Savina, A. A.; Abakumova, T. A.; Tendeloo, G. V.; Bals, S. Grain Boundaries as a Diffusion-Limiting Factor in Lithium-Rich NMC Cathodes for High-Energy Lithium-Ion Batteries. *ACS Applied Energy Materials* **2021**, *4*, 6777−6786.
(90) Plimpton, S. Computational limits of classical molecular dynamics simulations. *Comput. Mater. Sci.* **1995**, *4*, 361−364.
(91) Monticelli, L.; Tieleman, D. P. Force fields for classical molecular dynamics. *Methods Mol. Biol.* **2013**, *924*, 197−213.
(92) Sutmann, G. Classical molecular dynamics. In *Quantum simulations of complex many-body systems: from theory to algorithms*; Grotendorst, J., Marx, D., Muramatsu, A., Eds.; Universitat Stuttgart, 2002; Vol. *10*, pp 211−254

https://doi.org/10.1021/acsenergylett.1c02028
ACS Energy Lett. 2022, 7, 108−122

(93) Brooks, C. L., III; Case, D. A.; Plimpton, S.; Roux, B.; Van Der Spoel, D.; Tajkhorshid, E. Classical molecular dynamics. *J. Chem. Phys.* **2021**, *154*, 100401.
(94) Buckingham, R. A. The classical equation of state of gaseous helium, neon and argon. *Proc. R. Soc. London A: Mathematical and Physical Sciences* **1938**, *168*, 264−283.
(95) Born, M.; Mayer, J. On the Lattice Theory of Ionic Crystals. *Eur. Phys. J. A* **1932**, *75*, 1−18.
(96) Mayer, J. E. Dispersion and Polarizability and the Van der Waals Potential in the Alkali Halides. *J. Chem. Phys.* **1933**, *1*, 270.
(97) Mitchell, P. J.; Fincham, D. Shell model simulations by adiabatic dynamics. *J. Phys.: Condens. Matter* **1993**, *5*, 1031−1038.
(98) Escribano, B.; Lozano, A.; Radivojević, T.; Fernández-Pendás, M.; Carrasco, J.; Akhmatskaya, E. Enhancing sampling in atomistic simulations of solid-state materials for batteries: a focus on olivine $NaFePO_4$. *Theor. Chem. Acc.* **2017**, *136*, 43.
(99) Hart, F. X.; Bates, J. B. Lattice model calculation of the strain energy density and other properties of crystalline $LiCoO_2$. *J. Appl. Phys.* **1998**, *83*, 7560−7566.
(100) Fisher, C. A. J.; Saiful Islam, M.; Moriwake, H. Atomic Level Investigations of Lithium Ion Battery Cathode Materials. *J. Phys. Soc. Jpn.* **2010**, *79*, 59−64.
(101) Kerisit, S.; Chaka, A. M.; Droubay, T. C.; Ilton, E. S. Shell Model for Atomistic Simulation of Lithium Diffusion in Mixed Mn/Ti Oxides. *J. Phys. Chem. C* **2014**, *118*, 24231−24239.
(102) He, J.; Zhang, L.; Liu, L. Thermal transport in monocrystalline and polycrystalline lithium cobalt oxide. *Phys. Chem. Chem. Phys.* **2019**, *21*, 12192−12200.
(103) Plimpton, S. Fast Parallel Algorithms for Short-Range Molecular Dynamics. *J. Comput. Phys.* **1995**, *117*, 1−19.
(104) Todorov, I. T.; Smith, W.; Trachenko, K.; Dove, M. T. DL_POLY_3: new dimensions in molecular dynamics simulations via massive parallelism. *J. Mater. Chem.* **2006**, *16*, 1911−1918.
(105) Yang, H.; Savory, C. N.; Morgan, B. J.; Scanlon, D. O.; Skelton, J. M.; Walsh, A. Chemical Trends in the Lattice Thermal Conductivity of Li (Ni,Mn,Co) O2 (NMC) Battery Cathodes. *Chem. Mater.* **2020**, *32*, 7542−7550.
(106) Woodley, S. M.; Battle, P. D.; Catlow, C. R. A.; Gale, J. D. Development of a new interatomic potential for the modeling of ligand field effects. *J. Phys. Chem. B* **2001**, *105*, 6824−6830.
(107) Lee, S.; Park, S. S. Atomistic Simulation Study of Mixed-Metal Oxide ($LiNi_{1/3}Co_{1/3}Mn_{1/3}O_2$) Cathode Material for Lithium Ion Battery. *J. Phys. Chem. C* **2012**, *116*, 6484−6489.
(108) Nakamura, T.; Gao, H.; Ohta, K.; Kimura, Y.; Tamenori, Y.; Nitta, K.; Ina, T.; Oishi, M.; Amezawa, K. Defect chemical studies on oxygen release from the Li-rich cathode material $Li_{1.2}Mn_{0.6}Ni_{0.2}O_{2-\delta}$. *J. Mater. Chem. A* **2019**, *7*, 5009−5019.
(109) Kim, S. J.; Martinez-Lope, M. J.; Fernandez-Diaz, M. T.; Alonso, J. A.; Presniakov, I.; Demazeau, G. Evidence of Ni(III) Disproportionation in the $TlNiO_3$ Perovskite Lattice through Neutron Powder Diffraction and Mössbauer Spectroscopy. *Chem. Mater.* **2002**, *14*, 4926−4932.
(110) Alonso, J. A.; Martínez-Lope, M. J.; Casais, M. T.; Aranda, M. A. G.; Fernández-Díaz, M. T. Metal-Insulator Transitions, Structural and Microstructural Evolution of $RNiO_3$ (R = Sm, Eu, Gd, Dy, Ho, Y) Perovskites: Evidence for Room-Temperature Charge Disproportionation in Monoclinic $HoNiO_3$ and $YNiO_3$. *J. Am. Chem. Soc.* **1999**, *121*, 4754−4762.
(111) Lewis, G. V.; Catlow, C. R. A. Potential models for ionic oxides. *J. Phys. C: Solid State Phys.* **1985**, *18*, 1149−1161.
(112) Ledwaba, R. S.; Sayle, D. C.; Ngoepe, P. E. Atomistic Simulation and Characterization of Spinel $Li_{1+x}Mn_2O_4$ ($0 \leq x \leq 1$) Nanoparticles. *ACS Applied Energy Materials* **2020**, *3*, 1429−1438.
(113) Sayle, T. X. T.; Catlow, C. R. A.; Maphanga, R. R.; Ngoepe, P. E.; Sayle, D. C. Generating MnO_2 Nanoparticles Using Simulated Amorphization and Recrystallization. *J. Am. Chem. Soc.* **2005**, *127*, 12828−12837.
(114) Dawson, J. A.; Tanaka, I. Oxygen Vacancy Formation and Reduction Properties of β-MnO_2 Grain Boundaries and the Potential for High Electrochemical Performance. *ACS Appl. Mater. Interfaces* **2014**, *6*, 17776−17784.
(115) Ammundsen, B.; Burns, G. R.; Islam, M. S.; Kanoh, H.; Rozière, J. Lattice Dynamics and Vibrational Spectra of Lithium Manganese Oxides: A Computer Simulation and Spectroscopic Study. *J. Phys. Chem. B* **1999**, *103*, 5175−5180.
(116) Gale, J. D. GULP: A computer program for the symmetry-adapted simulation of solids. *J. Chem. Soc., Faraday Trans.* **1997**, *93*, 629−637.
(117) Pedone, A.; Malavasi, G.; Menziani, M. C.; Cormack, A. N.; Segre, U. A New Self-Consistent Empirical Interatomic Potential Model for Oxides, Silicates, and Silica-Based Glasses. *J. Phys. Chem. B* **2006**, *110*, 11780−11795.
(118) Nakamura, K.; Ohno, H.; Okamura, K.; Michihiro, Y.; Nakabayashi, I.; Kanashiro, T. On the diffusion of Li^+ defects in $LiCoO_2$ and $LiNiO_2$. *Solid State Ionics* **2000**, *135*, 143−147.
(119) Bruce, P.; Lisowska-Oleksiak, A.; Saidi, M.; Vincent, C. Vacancy diffusion in the intercalation electrode $Li_{1-x}NiO_2$. *Solid State Ionics* **1992**, *57*, 353−358.
(120) Gale, J. D. Empirical potential derivation for ionic materials. *Philos. Mag. B* **1996**, *73*, 3−19.
(121) de Tomas, C.; Suarez-Martinez, I.; Marks, N. A. Graphitization of amorphous carbons: A comparative study of interatomic potentials. *Carbon* **2016**, *109*, 681−693.
(122) Deringer, V. L.; Merlet, C.; Hu, Y.; Lee, T. H.; Kattirtzi, J. A.; Pecher, O.; Csányi, G.; Elliott, S. R.; Grey, C. P. Towards an atomistic understanding of disordered carbon electrode materials. *Chem. Commun.* **2018**, *54*, 5988−5991.
(123) Powles, R.; Marks, N.; Lau, D. Self-assembly of sp^2-bonded carbon nanostructures from amorphous precursors. *Phys. Rev. B: Condens. Matter Mater. Phys.* **2009**, *79*, 075430.
(124) Artrith, N.; Urban, A.; Ceder, G. Constructing first-principles phase diagrams of amorphous Li_xSi using machine-learning-assisted sampling with an evolutionary algorithm. *J. Chem. Phys.* **2018**, *148*, 241711.
(125) Onat, B.; Cubuk, E. D.; Malone, B. D.; Kaxiras, E. Implanted neural network potentials: Application to Li-Si alloys. *Phys. Rev. B: Condens. Matter Mater. Phys.* **2018**, *97*, 094106.
(126) Houchins, G.; Viswanathan, V. An accurate machine-learning calculator for optimization of Li-ion battery cathodes. *J. Chem. Phys.* **2020**, *153*, 054124.
(127) Wang, C.; Aoyagi, K.; Wisesa, P.; Mueller, T. Lithium ion conduction in cathode coating materials from on-the-fly machine learning. *Chem. Mater.* **2020**, *32*, 3741−3752.
(128) Artrith, N.; Morawietz, T.; Behler, J. High-dimensional neural-network potentials for multicomponent systems: Applications to zinc oxide. *Phys. Rev. B: Condens. Matter Mater. Phys.* **2011**, *83*, 153101.
(129) Faraji, S.; Ghasemi, S. A.; Rostami, S.; Rasoulkhani, R.; Schaefer, B.; Goedecker, S.; Amsler, M. High accuracy and transferability of a neural network potential through charge equilibration for calcium fluoride. *Phys. Rev. B: Condens. Matter Mater. Phys.* **2017**, *95*, 104105.
(130) Yang, H.; Yang, J.-Y.; Savory, C. N.; Skelton, J. M.; Morgan, B. J.; Scanlon, D. O.; Walsh, A. Highly anisotropic thermal transport in $LiCoO_2$. *J. Phys. Chem. Lett.* **2019**, *10*, 5552−5556.
(131) Takahata, K.; Terasaki, I. Thermal conductivity of $AxBO_2$-type layered oxides $Na_{0.77}MnO_2$ and $LiCoO_2$. *Jpn. J. Appl. Phys.* **2002**, *41*, 763.
(132) Chen, S.-C.; Wang, Y.-Y.; Wan, C.-C. Thermal analysis of spirally wound lithium batteries. *J. Electrochem. Soc.* **2006**, *153*, A637−A648.
(133) Feng, T.; O'Hara, A.; Pantelides, S. T. Quantum prediction of ultra-low thermal conductivity in lithium intercalation materials. *Nano Energy* **2020**, *75*, 104916.
(134) Xia, Y.; Hegde, V. I.; Pal, K.; Hua, X.; Gaines, D.; Patel, S.; He, J.; Aykol, M.; Wolverton, C. High-Throughput Study of Lattice Thermal Conductivity in Binary Rocksalt and Zinc Blende Compounds Including Higher-Order Anharmonicity. *Phys. Rev. X* **2020**, *10*, 041029.

https://doi.org/10.1021/acsenergylett.1c02028
ACS Energy Lett. 2022, 7, 108−122

(135) Kim, G. H.; Smith, K.; Lee, K. J.; Santhanagopalan, S.; Pesaran, A. Multi-Domain Modeling of Lithium-Ion Batteries Encompassing Multi-Physics in Varied Length Scales. *J. Electrochem. Soc.* **2011**, *158*, A955−A969.
(136) Jin, N.; Danilov, D. L.; Van den Hof, P. M.; Donkers, M. Parameter estimation of an electrochemistry-based lithium-ion battery model using a two-step procedure and a parameter sensitivity analysis. *Int. J. Energy Res.* **2018**, *42*, 2417−2430.
(137) Marquis, S. G.; Sulzer, V.; Timms, R.; Please, C. P.; Chapman, S. J. An Asymptotic Derivation of a Single Particle Model with Electrolyte. *J. Electrochem. Soc.* **2019**, *166*, A3693−A3706.
(138) Krewer, U.; Röder, F.; Harinath, E.; Braatz, R. D.; Bedürftig, B.; Findeisen, R. Review—Dynamic Models of Li-Ion Batteries for Diagnosis and Operation: A Review and Perspective. *J. Electrochem. Soc.* **2018**, *165*, A3656−A3673.
(139) Richardson, G.; Korotkin, I.; Ranom, R.; Castle, M.; Foster, J. M. Generalised single particle models for high-rate operation of graded lithium-ion electrodes: Systematic derivation and validation. *Electrochim. Acta* **2020**, *339*, 135862.
(140) Kindermann, F. M.; Keil, J.; Frank, A.; Jossen, A. A SEI Modeling Approach Distinguishing between Capacity and Power Fade. *J. Electrochem. Soc.* **2017**, *164*, e287−e294.
(141) Sturm, J.; Ludwig, S.; Zwirner, J.; Ramirez-Garcia, C.; Heinrich, B.; Horsche, M. F.; Jossen, A. Suitability of physicochemical models for embedded systems regarding a nickel-rich, silicon-graphite lithium-ion battery. *J. Power Sources* **2019**, *436*, 226834.
(142) Ecker, M.; Tran, T. K. D.; Dechent, P.; Käbitz, S.; Warnecke, A.; Sauer, D. U. Parameterization of a Physico-Chemical Model of a Lithium-Ion Battery. *J. Electrochem. Soc.* **2015**, *162*, A1836−A1848.
(143) Stewart, S. G.; Srinivasan, V.; Newman, J. Modeling the Performance of Lithium-Ion Batteries and Capacitors during Hybrid-Electric-Vehicle Operation. *J. Electrochem. Soc.* **2008**, *155*, A664.
(144) Schmalstieg, J.; Rahe, C.; Ecker, M.; Sauer, D. U. Full Cell Parameterization of a High-Power Lithium-Ion Battery for a Physico-Chemical Model: Part I. Physical and Electrochemical Parameters. *J. Electrochem. Soc.* **2018**, *165*, a3799−a3810.
(145) Liebig; Gupta; Kirstein; Schuldt; Agert. Parameterization and Validation of an Electrochemical Thermal Model of a Lithium-Ion Battery. *Batteries* **2019**, *5*, 62.
(146) Viswanathan, V. V.; Choi, D.; Wang, D.; Xu, W.; Towne, S.; Williford, R. E.; Zhang, J.-G.; Liu, J.; Yang, Z. Effect of entropy change of lithium intercalation in cathodes and anodes on Li-ion battery thermal management. *J. Power Sources* **2010**, *195*, 3720−3729.
(147) Lu, X.; Bertei, A.; Finegan, D. P.; Tan, C.; Daemi, S. R.; Weaving, J. S.; O'Regan, K. B.; Heenan, T. M. M.; Hinds, G.; Kendrick, E.; Brett, D. J. L.; Shearing, P. R. 3D microstructure design of lithium-ion battery electrodes assisted by X-ray nano-computed tomography and modelling. *Nat. Commun.* **2020**, *11*, 2079.
(148) Amin, R.; Chiang, Y.-M. Characterization of Electronic and Ionic Transport in $Li_{1-x}Ni_{0.33}Mn_{0.33}Co_{0.33}O_2$(NMC333) and $Li_{1-x}Ni_{0.50}Mn_{0.20}Co_{0.30}O_2$(NMC523) as a Function of Li Content. *J. Electrochem. Soc.* **2016**, *163*, A1512−A1517.
(149) Jung, R.; Metzger, M.; Maglia, F.; Stinner, C.; Gasteiger, H. A. Oxygen release and its effect on the cycling stability of $LiNi_xMn_yCo_zO_2$ (NMC) cathode materials for Li-ion batteries. *J. Electrochem. Soc.* **2017**, *164*, A1361.
(150) Chen, C.-H.; Planella, F. B.; O'Regan, K.; Gastol, D.; Widanage, W. D.; Kendrick, E. Development of Experimental Techniques for Parameterization of Multi-scale Lithium-ion Battery Models. *J. Electrochem. Soc.* **2020**, *167*, 080534.
(151) Sturm, J.; Rheinfeld, A.; Zilberman, I.; Spingler, F. B.; Kosch, S.; Frie, F.; Jossen, A. Modeling and simulation of inhomogeneities in a 18650nickel -rich,silicon -graphitelithium -ioncell during fast charging. *J. Power Sources* **2019**, *412*, 204−223.
(152) Tranter, T. G.; Timms, R.; Heenan, T. M. M.; Marquis, S. G.; Sulzer, V.; Jnawali, A.; Kok, M. D. R.; Please, C. P.; Chapman, S. J.; Shearing, P. R.; et al. Probing Heterogeneity in Li-Ion Batteries with Coupled Multiscale Models of Electrochemistry and Thermal Transport using Tomographic Domains. *J. Electrochem. Soc.* **2020**, *167*, 110538.
(153) Tranter, T. G.; Timms, R.; Shearing, P. R.; Brett, D. J. L. Communication—Prediction of Thermal Issues for Larger Format 4680 Cylindrical Cells and Their Mitigation with Enhanced Current Collection. *J. Electrochem. Soc.* **2020**, *167*, 160544.
(154) Wang, A. *LiionDB*; http://www.liiondb.com (accessed 01-12-21).
(155) Sulzer, V.; Marquis, S. G.; Timms, R.; Robinson, M.; Chapman, S. J. Python Battery Mathematical Modelling (PyBaMM). *Journal of Open Research Software* **2021**, *9*, 14.
(156) Chen, C.-H.; Brosa Planella, F.; O'Regan, K.; Gastol, D.; Widanage, W. D.; Kendrick, E. *Experimental data for "Development of Experimental Techniques for Parameterization of Multi-scale Lithium-ion Battery Models"*, May 15, 2020; https://zenodo.org/record/4032561#.X3RFuWhKiUl.
(157) Devie, A.; Baure, G.; Dubarry, M. Intrinsic Variability in the Degradation of a Batch of Commercial 18650Lithium -IonCells. *Energies* **2018**, *11*, 1031.
(158) *Battery Archive: A repository for easy visualization, analysis, and comparison of battery data across institutions*; https://www.batteryarchive.org (accessed 01-11-21).
(159) Edge, J. S.; O'Kane, S.; Prosser, R.; Kirkaldy, N. D.; Patel, A. N.; Hales, A.; Ghosh, A.; Ai, W.; Chen, J.; Yang, J.; Li, S.; Pang, M.-C.; Bravo Diaz, L.; Tomaszewska, A.; Marzook, M. W.; Radhakrishnan, K. N.; Wang, H.; Patel, Y.; Wu, B.; Offer, G. J.; et al. Lithium ion battery degradation: what you need to know. *Phys. Chem. Chem. Phys.* **2021**, *23*, 8200−8221.
(160) Erickson, E. M.; Schipper, F.; Penki, T. R.; Shin, J.-Y.; Erk, C.; Chesneau, F.-F.; Markovsky, B.; Aurbach, D. Recent advances and remaining challenges for lithium ion battery cathodes. *J. Electrochem. Soc.* **2017**, *164*, A6341.
(161) Woodford, W. H.; Chiang, Y.-M.; Carter, W. C. Electrochemical shock" of intercalation electrodes: a fracture mechanics analysis. *J. Electrochem. Soc.* **2010**, *157*, A1052.
(162) Jung, R.; Metzger, M.; Maglia, F.; Stinner, C.; Gasteiger, H. A. Chemical versus electrochemical electrolyte oxidation on NMC111, NMC622, NMC811, LNMO, and conductive carbon. *J. Phys. Chem. Lett.* **2017**, *8*, 4820−4825.
(163) Phillip, N. D.; Westover, A. S.; Daniel, C.; Veith, G. M. Structural Degradation of High Voltage Lithium Nickel Manganese Cobalt Oxide (NMC) Cathodes in Solid-State Batteries and Implications for Next Generation Energy Storage. *ACS Applied Energy Materials* **2020**, *3*, 1768−1774.
(164) Li, D.; Li, H.; Danilov, D.; Gao, L.; Zhou, J.; Eichel, R.-A.; Yang, Y.; Notten, P. H. Temperature-dependent cycling performance and ageing mechanisms of $C_6/LiNi_{1/3}Mn_{1/3}Co_{1/3}O_2$ batteries. *J. Power Sources* **2018**, *396*, 444−452.
(165) Billy, E.; Joulié, M.; Laucournet, R.; Boulineau, A.; De Vito, E.; Meyer, D. Dissolution mechanisms of $LiNi_{1/3}Mn_{1/3}Co_{1/3}O_2$ positive electrode material from lithium-ion batteries in acid solution. *ACS Appl. Mater. Interfaces* **2018**, *10*, 16424−16435.
(166) Reniers, J. M.; Mulder, G.; Howey, D. A. Review and performance comparison of mechanical-chemical degradation models for lithium-ion batteries. *J. Electrochem. Soc.* **2019**, *166*, A3189.
(167) Jana, A.; Shaver, G. M.; García, R. E. Physical, on the fly, capacity degradation prediction of $LiNiMnCoO_2$-graphite cells. *J. Power Sources* **2019**, *422*, 185−195.
(168) Lin, X.; Park, J.; Liu, L.; Lee, Y.; Sastry, A.; Lu, W. A comprehensive capacity fade model and analysis for Li-ion batteries. *J. Electrochem. Soc.* **2013**, *160*, A1701.
(169) Ghosh, A.; Foster, J. M.; Offer, G.; Marinescu, M. A Shrinking-Core Model for the Degradation of High-Nickel Cathodes (NMC811) in Li-Ion Batteries: Passivation Layer Growth and Oxygen Evolution. *J. Electrochem. Soc.* **2021**, *168*, 020509.
(170) Dai, Y.; Cai, L.; White, R. E. Capacity fade model for spinel $LiMn_2O_4$ electrode. *J. Electrochem. Soc.* **2013**, *160*, A182.
(171) Fackeldey, K. Challenges in Atomistic-to-Continuum Coupling. *Math. Probl. Eng.* **2015**, *2015*, 1−10.

https://doi.org/10.1021/acsenergylett.1c02028
ACS Energy Lett. 2022, 7, 108−122

(172) Badia, S.; Bochev, P.; Gunzburger, M.; Lehoucq, R.; Parks, M. *International Conference on Large-Scale Scientific Computing*, 2007; pp 16 − 27.

https://doi.org/10.1021/acsenergylett.1c02028
ACS Energy Lett. 2022, 7, 108−122